Multifunctional ginsenoside Rg3-integrated liposomes for synergistic chemo-photothermal-immunotherapy against multidrug-resistant breast cancer

Wuyan Xie, [a] *Kai Wang,* [a] *Qin Zhou,* [a] *Haihua Zhou,* [c] *Qing Zhu,* [a*] *Dan Wu* [b*] *& Wei Shen* [c*]

[a] State Key Laboratory of Green Chemical Synthesis and Conversion, Hangzhou 310014, China.

[b] College of Materials Science and Engineering, Zhejiang University of Technology, Hangzhou 310014, P. R. China.

[c] Department of Surgery, Affiliated Jinhua Hospital, Zhejiang University School of Medicine, Jinhua 321000, China.

[*]Corresponding authors: shenweiri@163.com (W. Shen), danwu@zjut.edu.cn (D. Wu), zhuq@zjut.edu.cn (Q. Zhu)

Experimental methods

In vitro stability evaluation of the liposomes

The CID-LPs and RID-LPs solutions prepared with the optimal formulation were stored at room temperature and at 4℃. Their particle size and polydispersity index (PDI) were measured on days 1, 2, 3, 4, 5, 6, and 7 to evaluate the storage stability of the two liposomes.

Freshly prepared CID-LPs and RID-LPs solutions were mixed with an equal volume of DMEM containing 10% FBS and incubated at 37℃. Samples were taken at 0, 1, 2, 4, 6, 8, 10, 12, 24, and 48 h, and their particle size and PDI were measured to assess the serum stability of the two liposomes.

In vitro release study of the liposomes

The *in vitro* release profiles of ICG and DDP were determined using a dialysis method. The procedure was as follows: 1.0 mL of CID-LPs and RID-LPs solutions were each placed into dialysis bags with a MWCO of 3500 Da and sealed. The bags were then immersed in release containers containing 40 mL of PBS buffer (pH 7.4) with 0.5% (v/v) Tween 80. The release conditions were kept identical for both ICG and DDP to maintain a consistent comparison framework. All release experiments were conducted in triplicate (n=3) at 37℃ with a shaking speed of 100 rpm. At 0.5, 1, 2, 4, 6, 8, 12, 24, 36, and 48 h, 1 mL of release medium was withdrawn and replaced with an equal volume of fresh medium. The concentrations of released ICG and DDP were quantified by HPLC, and the cumulative drug release percentages were calculated.

Photothermal stability of RID-LPs

RID-LPs samples at a concentration of 5.0 μg/mL (DDP equivalent) were subjected to repeated on/off irradiation cycles under an 808 nm laser at power densities of 0.5, 1.0, and 1.5 W/cm^2. Each cycle consisted of 4 minutes of irradiation followed by 11 minutes without irradiation, for a total

of 5 cycles (75 minutes in total). Temperature changes were continuously monitored and recorded in real time using an infrared thermal imager.

Photothermal conversion efficiency of RID-LPs

The photothermal conversion efficiency of RID-LPs was calculated according to the method reported in the literature.[1,2] Briefly, RID-LPs samples at a working concentration of 5.0 μg/mL (DDP equivalent) were continuously irradiated with an 808 nm laser at a power density of 1.0 W/cm^2 for 4 minutes, followed by natural cooling for 11 minutes after the laser was turned off. Temperature changes during both the heating and cooling processes were monitored and recorded in real time using an infrared thermal imager. The photothermal conversion efficiency (η) was then calculated using the following Equation (1):

$$\eta=[hs(T_{Max}-T_{Surr})-Q_{Dis}]/[I(1-10^{-A808})] \quad (1)$$

Where h is the heat transfer coefficient; S is the surface area of the container; T_{Max} and T_{Surr} represent the maximum steady-state temperature of the system and the ambient temperature, respectively; Q_{Dis} indexes the heat dissipated by the solvent and container, which was determined using PBS buffer (pH 7.4); I is the laser power density (1.0 W/cm^2), and A_{808} represents the absorbance of RID-LPs at 808 nm. The parameter hS can be calculated according to Equation (2):

$$hs=m_D C_D/\tau_s \quad (2)$$

Where m_D is the mass of the RID-LPs solution; C_D represents the specific heat capacity of the solution; and τ_s is the corresponding time constant, which can be calculated according to Equation (3):

$$\tau_s=-\ln\theta/t \quad (3)$$

Where t represents the natural cooling time of the system after the laser is turned off; and θ is a dimensionless parameter, known as the driving force temperature, which can be calculated according to Equation (4):

$$\theta=(T-T_{Surr})/(T_{Max}-T_{Surr}) \quad (4)$$

Where *T* represents the real-time temperature during the cooling period.

Western blot analysis of P-glycoprotein (P-gp) expression

To investigate the impact of ginsenoside Rg3 on P-gp expression, MCF-7/DDP cells were seeded into 12-well plates at a density of 1.6×10^5 cells per well and cultured for 24 h to allow for cell attachment. The cells were then divided into two groups: a control group and an Rg3-treated group (10 μg/mL of Rg3 for 24 h). Following the treatment, the cells were washed with ice-cold PBS and lysed using RIPA buffer containing protease inhibitors to extract total proteins. The protein concentration of each sample was determined using a BCA Protein Assay Kit to ensure uniform loading. Equal amounts of protein (20 μg per lane) were separated by 10% SDS-PAGE and then transferred onto PVDF membranes. The membranes were blocked with 5% non-fat milk in TBST for 2 h at room temperature to prevent non-specific binding. After blocking, the membranes were incubated separately overnight at 4℃ with primary antibodies against P-gp and GAPDH, respectively. After washing with TBST, the membranes were incubated with the corresponding HRP-conjugated secondary antibodies for 1.5 h at room temperature. Finally, the protein bands were visualized using an ECL Detection Kit and quantified with ImageJ software (version 1.53q, National Institutes of Health, USA), with P-gp expression levels normalized to GAPDH as the internal loading control.

Intracellular accumulation assay of P-gp substrates

To investigate the inhibitory effect of Rg3 on P-gp-mediated efflux, MCF-7/DDP cells were seeded into confocal dishes at a density of 1.2×10^5 cells per dish and cultured for 24 h to allow attachment. The cells were then pre-treated with or without Rg3 (10 μg/mL) for 8 h to ensure sufficient interaction with P-gp. After this treatment, the cells were incubated separately with one of the three P-gp substrates, including Rh123, Calcein-AM, or DOX, at a concentration of 10 μM

for 0.5 h at 37°C. Following incubation, the cells were washed three times with PBS (pH 7.4) and stained with Hoechst 33342 to label the nuclei. After a final wash, the samples were imaged using a confocal laser scanning microscope (Leica STELLARIS 5, Leica Microsystems, Germany).

UV–Vis absorption spectroscopy measurement

Free ICG, CID-LPs, and RID-LPs solutions were appropriately diluted to suitable concentrations, respectively. The absorption spectra of the samples were measured using a microplate reader (Synergy H1, BioTek Instruments, USA) by scanning over a wavelength range of 350-995 nm. The scanning interval was set to 5 nm, and the scanning speed was set to medium. All experiments were independently repeated three times. Finally, the absorbance-wavelength spectra were plotted using Origin software (version 2018, OriginLab Corporation, USA).

Permeation evaluation of liposomes in tumor spheroids

Tumor spheroids were generated in low-adhesion 96-well plates (SLP-U-96-ST, EXCELLENT BIOSCIENCES, China) by seeding 3×10^3 MCF-7/T cells per well and culturing for 7 days to obtain uniform three-dimensional structures. Subsequently, CID-LPs and RID-LPs were added to the spheroids at a concentration of 5.0 μg/mL (DDP equivalent) and incubated for an additional 8 h. After thorough washing with PBS (pH 7.4), Z-stack imaging was performed from the top to the bottom of the spheroids using a confocal laser scanning microscope (Leica STELLARIS 5, Leica Microsystems, Germany) to evaluate the spatial distribution of ICG fluorescence.

***In vitro* photothermal performance evaluation**

To evaluate the photothermal performance of liposomes at the cellular level, MCF-7/DDP cells were seeded into 96-well plates at a density of 1×10^4 cells per well and cultured for 24 h to allow cell attachment. The culture medium was then replaced with fresh PBS (pH 7.4), CID-LPs, or RID-LPs at a working concentration of 5.0 μg/mL (DDP equivalent), followed by an additional 4 h of incubation. Subsequently, the plate was irradiated with an 808 nm NIR laser at a power density

of 1.0 W/cm^2. During irradiation, the temperature was recorded every 30 s using an infrared thermal imager, and thermal images were captured every 1 min.

Wound healing assay

To evaluate the effects of different treatments on the migratory ability of MCF-7 and MCF-7/DDP cells, both cell lines were seeded in 6-well plates at a density of 5×10^5 cells per well and cultured for 24 h until a confluent monolayer was formed. A straight wound was created by scraping the cell layer with a sterile 200 μL pipette tip held perpendicular to the well bottom, followed by three gentle washes with PBS (pH 7.4) to remove detached cells. Images of the wounds were captured at 0 h before treatment, and cells were divided into four groups: the Control group with fresh basal medium, the DDP group with medium containing 5.0 μg/mL cisplatin, and the CID-LPs + L and RID-LPs + L groups with media containing 5.0 μg/mL (DDP equivalent) of CID-LPs or RID-LPs, respectively. After an additional 4 h of incubation, the CID-LPs + L and RID-LPs + L groups were irradiated with an 808 nm laser (1.0 W/cm^2) for 5 min. Cells were then cultured for a further 24 h, and wound images were taken at the same positions. The wound area was quantified using ImageJ software (version 1.53q, National Institutes of Health, USA), and the cell migration ratio was calculated according to Equation (5):

$$\text{Migration ratio}(\%)=(A_{0\,h}-A_{24\,h})/A_{0\,h}\times100\% \quad (5)$$

where $A_{0\,h}$ represents the wound area at 0 h, and $A_{24\,h}$ refers to the wound area at 24 h.

Lactate dehydrogenase (LDH) release assay

To assess the induction of pyroptosis, the release of LDH was measured using a commercial cytotoxicity assay kit according to the manufacturer's protocol. MCF-7 and MCF-7/DDP cells were seeded into 96-well plates at a density of 5×10^3 cells per well and cultured for 24 h. The cells were then treated with the different formulations at a working concentration of 5.0 μg/mL and divided into four groups: Control, DDP, CID-LPs + L, and RID-LPs + L. For the photothermal

groups (CID-LPs + L and RID-LPs + L), cells were irradiated with an 808 nm laser (1.0 W/cm^2, 5 min) after 4 h of incubation, while the non-irradiated groups were protected from light. After a total of 24 h, the culture plate was centrifuged at 400 g for 5 min, and the supernatant from each well was collected for the LDH assay. The supernatant was mixed with LDH assay buffer and NAD solution, followed by incubation at 37℃ for 15 min. Subsequently, dinitrophenylhydrazine solution was added and the mixture was incubated for another 15 min at 37℃. Finally, alkaline chromogen solution and distilled water were added to the mixture. After 5 min of stabilization at room temperature, the absorbance was measured at 440 nm using a microplate reader. The relative LDH release was calculated as the ratio of the absorbance of the sample group to that of the control group ($Abs_{Sample}/Abs_{Control}$).

Caspase-3 activity assay

To evaluate the effects of different treatments on apoptosis in MCF-7 and MCF-7/DDP cells, Caspase-3 activity was analyzed using an AFC-based Caspase-3 fluorometric assay kit. Both cell lines were seeded in 60 mm culture dishes at a density of 1.6×10^6 cells per dish and cultured for 24 h. The cells were then treated with the different formulations at a working concentration of 5.0 μg/mL and divided into four groups: Control, DDP, CID-LPs + L, and RID-LPs + L. For the photothermal groups (CID-LPs + L and RID-LPs + L), cells were irradiated with an 808 nm laser (1.0 W/cm^2, 5 min) after 4 h of incubation with the liposomes, while the Control and DDP groups were protected from light throughout the experiment. Cells were further cultured until 24 h, collected, and washed with PBS, then lysed on ice for 1 h using pre-chilled lysis buffer containing DTT. The lysates were centrifuged to collect the supernatant, and protein concentration was determined. An aliquot of lysate containing 150 μg protein was mixed with reaction buffer stock solution (containing DTT) and ddH_2O, followed by the addition of freshly prepared Caspase-3 substrate solution. The mixture was incubated at 37℃ in the dark for 1.5 h. Fluorescence intensity

was measured using a microplate reader (excitation: 485 nm, emission: 535 nm). PBS and reaction buffer were used as blank controls, and the relative Caspase-3 activity was calculated as the ratio of fluorescence intensity of the sample group to that of the control group ($RFU_{Sample}/RFU_{Control}$).

Hemolysis assay

Fresh whole blood was collected from healthy BALB/c mice into heparinized tubes and centrifuged at 10,000 r/min for 10 min at 4℃. The supernatant was discarded, and red blood cells (RBCs) were washed three times with PBS, then resuspended in PBS to obtain a 2% (w/v) RBC suspension. CID-LPs and RID-LPs were diluted with PBS to final concentrations of 160, 80, 40, 20, 10, 5, and 2.5 μg/mL (DDP equivalent). Equal volumes (100 μL) of RBC suspension and each liposome solution were mixed and incubated at 37℃ for 4 h. PBS and 1% Triton X-100 served as negative and positive controls, respectively. After incubation, samples were centrifuged at 5000 r/min for 5 min, and the absorbance of the supernatants was measured at 540 nm. Hemolysis rate was calculated according to Equation (6):

$$\text{Hemolysis}(\%)=(OD_{Sample}-OD_{Negative})/(OD_{Positive}-OD_{Negative})\times 100\% \quad (6)$$

Hematoxylin and Eosin (H&E) staining

At the endpoint of the antitumor therapy study (day 21), mice were euthanized by cervical dislocation under deep anesthesia with 3% isoflurane. Major organs, including the heart, liver, spleen, lungs, and kidneys, were immediately harvested, gently rinsed with pre-cooled PBS to remove residual blood, and fixed in 4% paraformaldehyde for 24 h. The fixed tissues were then embedded in paraffin, sectioned, and subjected to H&E staining for histopathological evaluation.

Supporting figures and tables

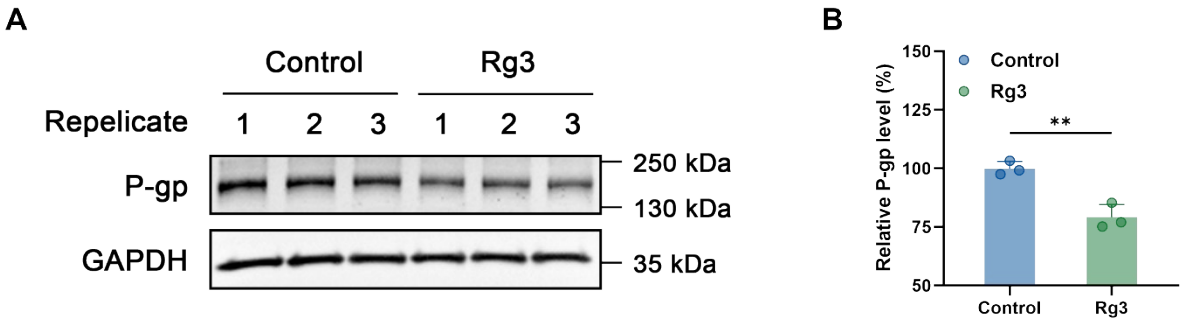

Figure S1. Rg3 downregulates P-gp protein expression in MCF-7/DDP cells. **A** Western blot images showing the protein levels of P-gp in MCF-7/DDP cells treated with or without Rg3. GAPDH was used as an internal loading control. **B** Quantitative analysis of P-gp protein levels normalized to GAPDH. (n=3) $^{**}p<0.01$; Data are presented as the mean ± SD from three independent experiments; Differences between two groups were assessed by an unpaired t-test, while comparisons among multiple groups were analyzed using one-way ANOVA.

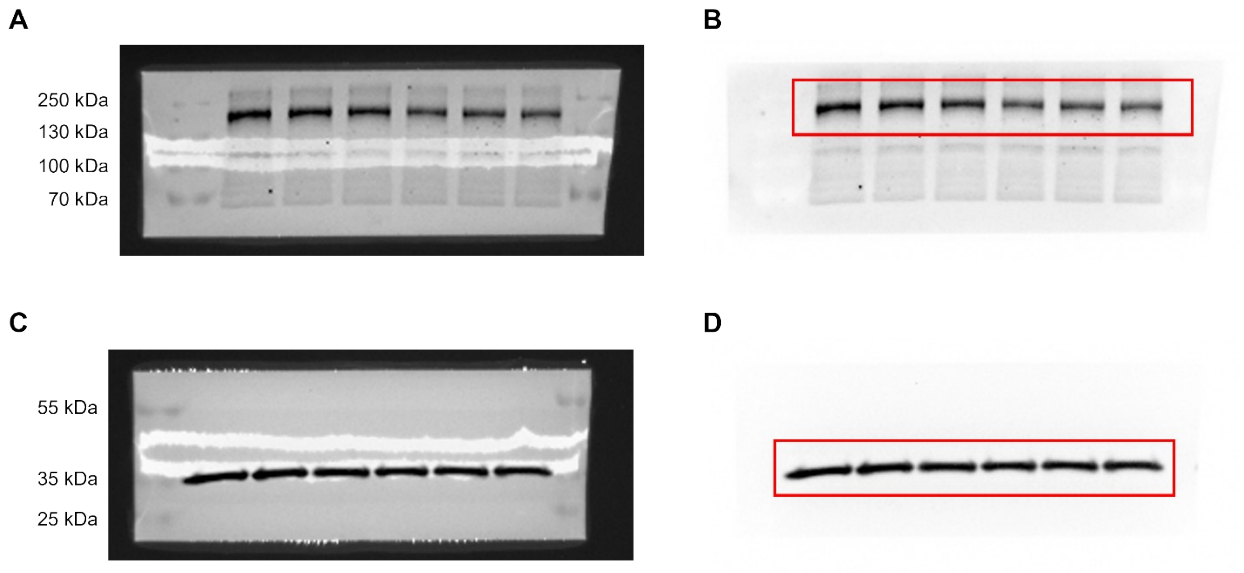

Figure S2. Original, uncropped Western blot images for P-gp and GAPDH. **A** Merged image of the brightfield (showing molecular weight markers) and chemiluminescent signal for P-gp. **B** Chemiluminescent image of P-gp. The red box indicates the specific area cropped for presentation in the main figure. **C** Merged image of the brightfield and chemiluminescent signal for GAPDH. **D** Chemiluminescent image of GAPDH. The red box indicates the area cropped for presentation in the main figure. All molecular weight markers are indicated on the left.

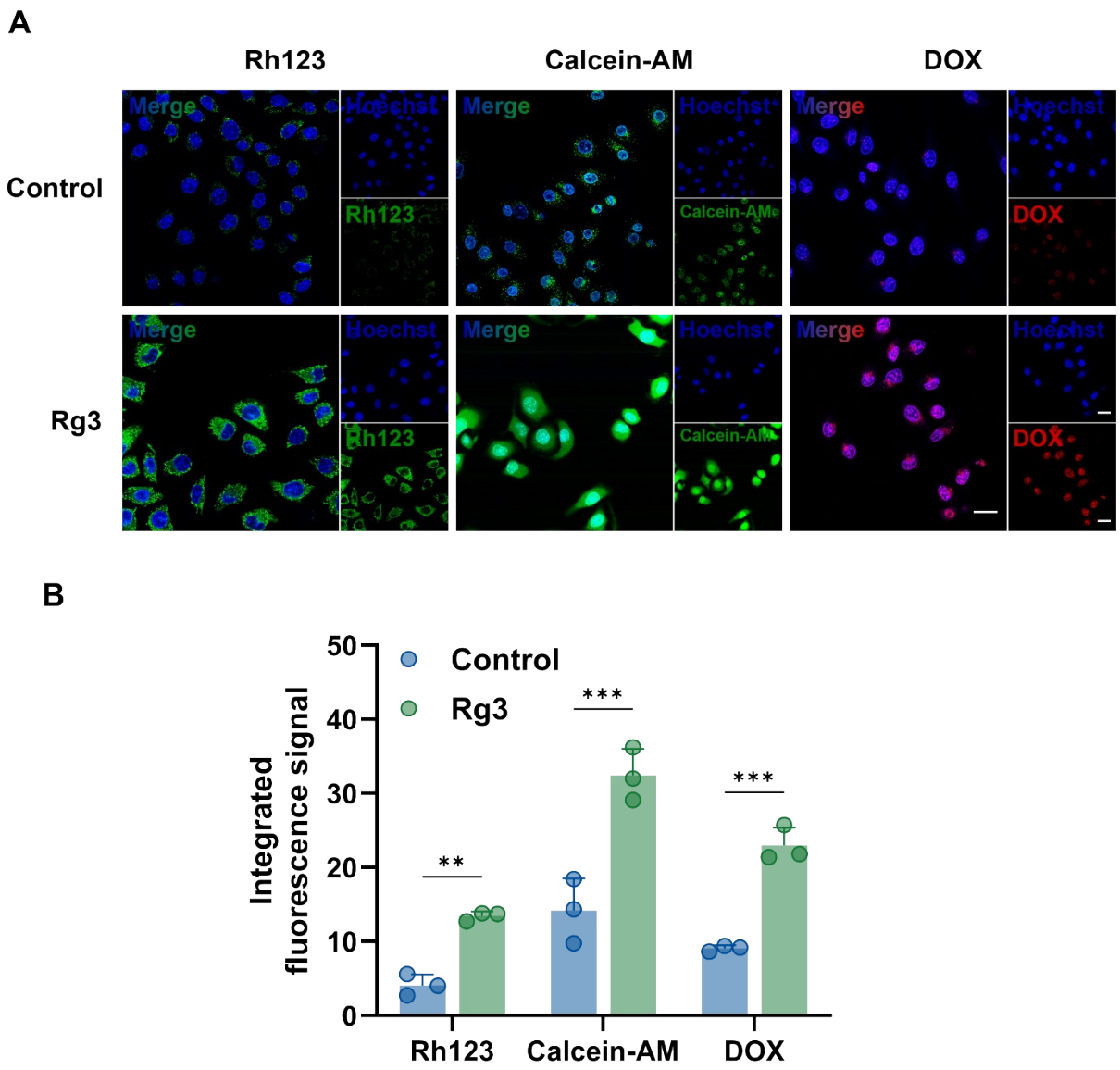

Figure S3. Rg3 inhibits P-gp-mediated efflux and increases intracellular substrate accumulation. **A** Confocal microscopy images showing the intracellular accumulation of P-gp substrates: Rh123 (green), Calcein-AM (green), and DOX (red) in MCF-7/DDP cells after treatment with or without Rg3. Nucleus were stained with Hoechst 33342 (blue). Scale bar: 25 μm. **B** Quantitative analysis of the integrated fluorescence intensity of Rh123, Calcein-AM, and DOX from confocal images. (n=3) $^{**}p<0.01$, and $^{***}p<0.001$; Data are presented as the mean ± SD from three independent experiments; Differences between two groups were assessed by an unpaired t-test, while comparisons among multiple groups were analyzed using one-way ANOVA.

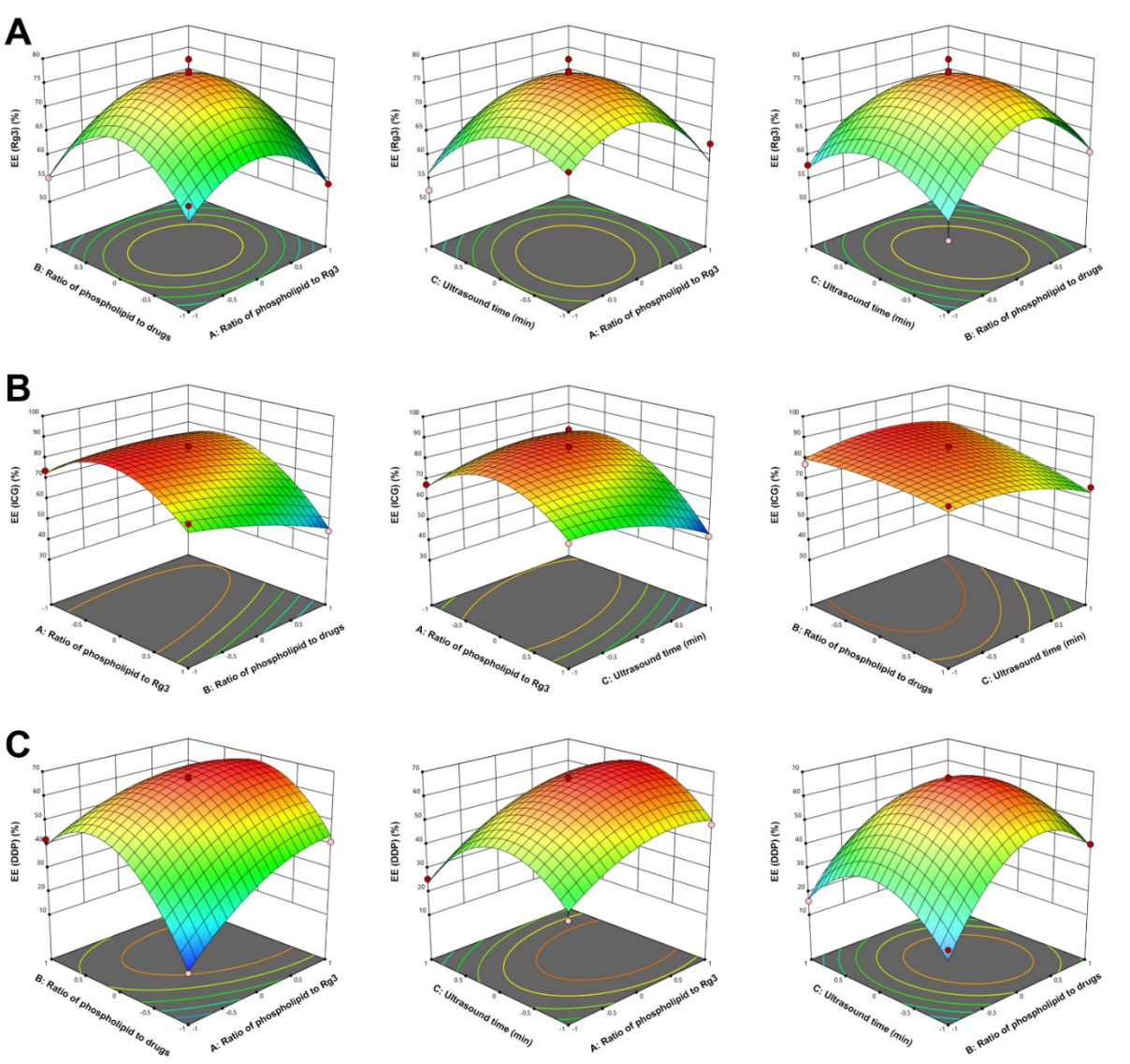

Figure S4. Optimization of formulation parameters using Box-Behnken design (BBD). **A-C** Response surface plots showing the effects of independent variables on the encapsulation efficiency (EE) of Rg3 (**A**), ICG (**B**), and DDP (**C**). The variables investigated are the ratio of phospholipid to Rg3, the ratio of phospholipid to drugs, and ultrasound time.

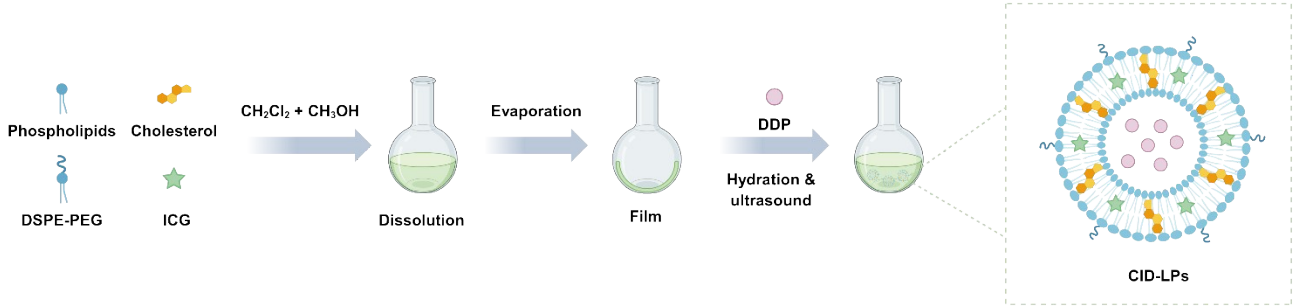

Figure S5. Schematic illustration of the preparation of CID-LPs via the thin-film hydration method.

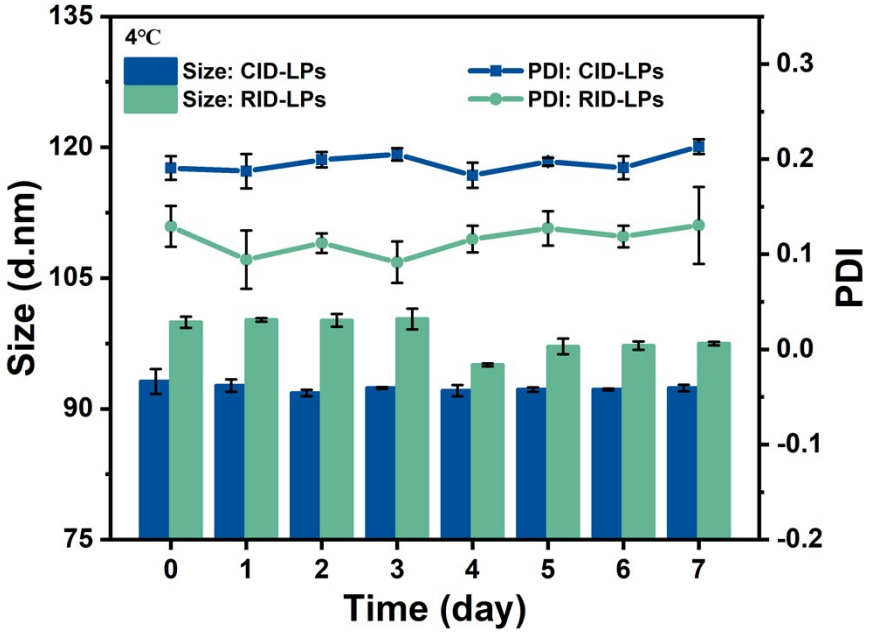

Figure S6. Stability evaluation of CID-LPs and RID-LPs stored at 4℃ for 7 days.

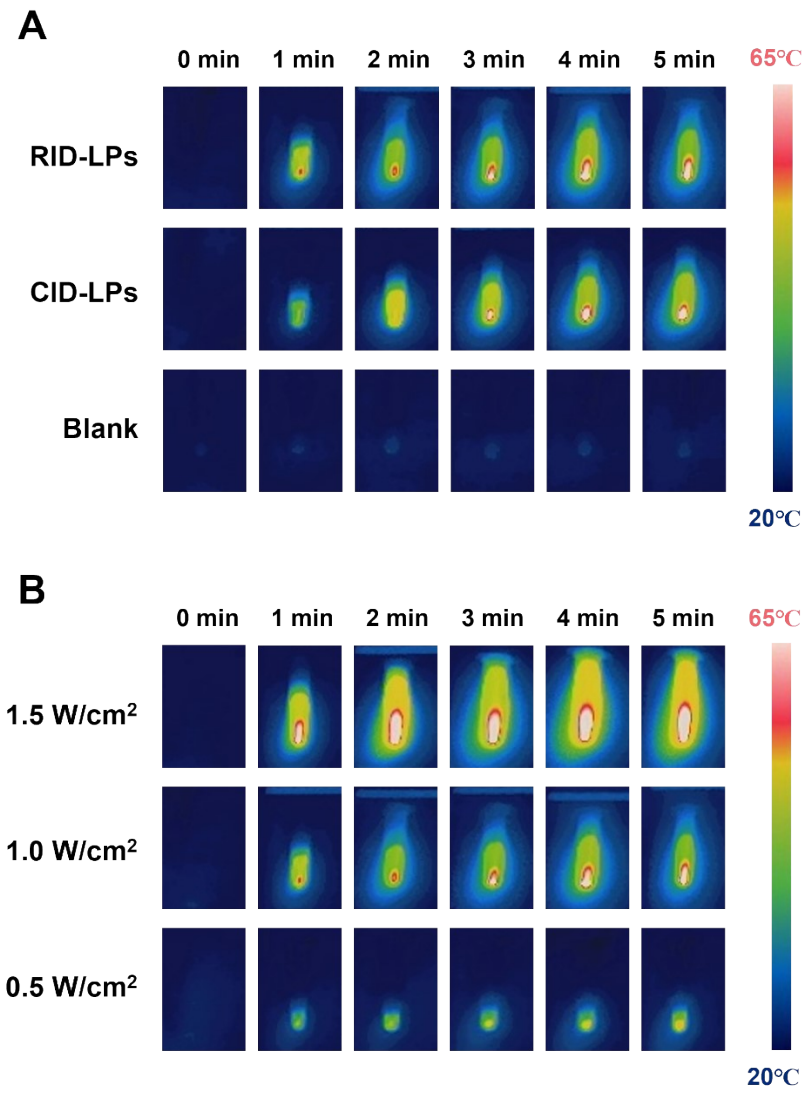

Figure S7. *In vitro* photothermal performance of liposomes. **A** Infrared thermal images of RID-LPs, CID-LPs, and blank control (PBS) under 808 nm laser irradiation (1.0 W/cm^2) over 5 min. **B** Infrared thermal images of RID-LPs under 808 nm laser irradiation at different power densities (0.5, 1.0, and 1.5 W/cm^2) over 5 min.

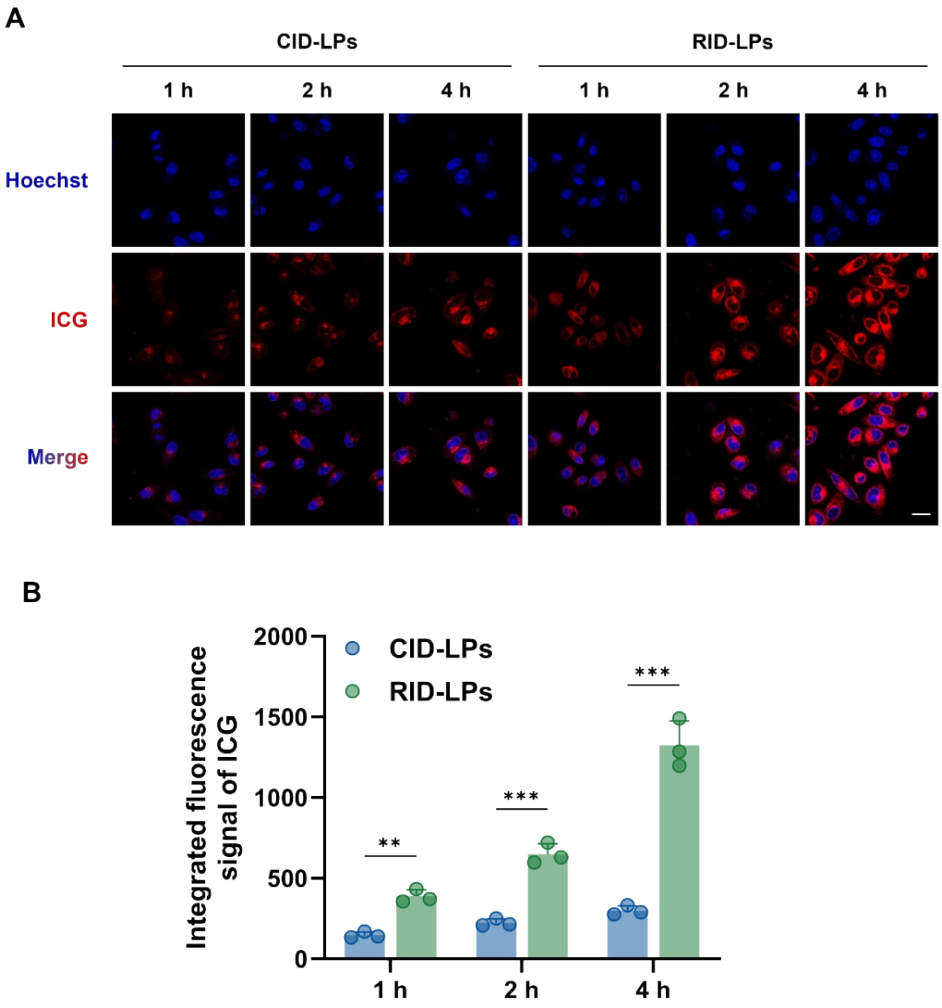

Figure S8. Time-dependent cellular uptake of CID-LPs and RID-LPs in MCF-7/DDP cells. **A** Representative confocal microscopy images showing intracellular distribution of Hoechst 33342 (blue, nucleus) and ICG (red) after 1, 2, and 4 h incubation with CID-LPs or RID-LPs (scale bar: 25 μm). **B** Quantitative analysis of the integrated fluorescence intensity of ICG from confocal images. (n=3) $^{**}p<0.01$, and $^{***}p<0.001$; Data are presented as the mean ± SD from three independent experiments; Differences between two groups were assessed by an unpaired t-test, while comparisons among multiple groups were analyzed using one-way ANOVA.

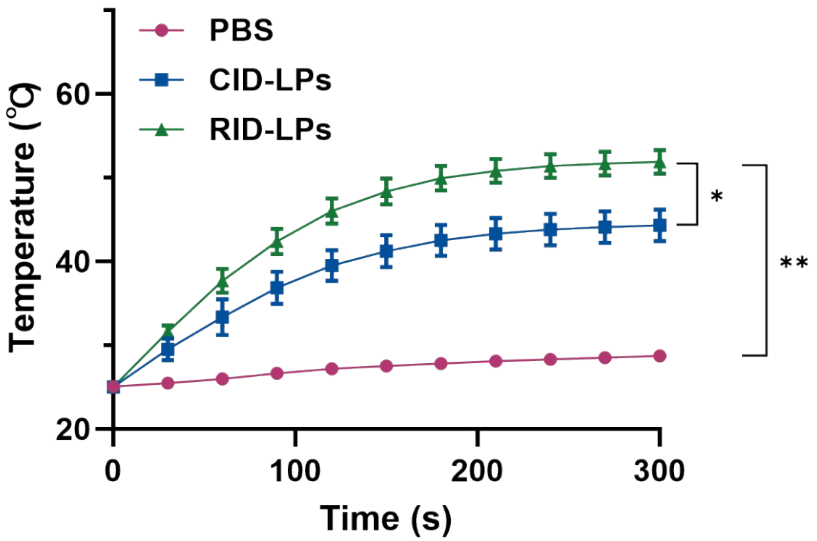

Figure S9. Photothermal heating curves of MCF-7/DDP cells treated with different formulations under 808 nm laser irradiation (1.0 W/cm^2). (n=3) *p<0.05, and **p<0.01; Data are presented as the mean ± SD from three independent experiments; Differences between two groups were assessed by an unpaired t-test, while comparisons among multiple groups were analyzed using one-way ANOVA.

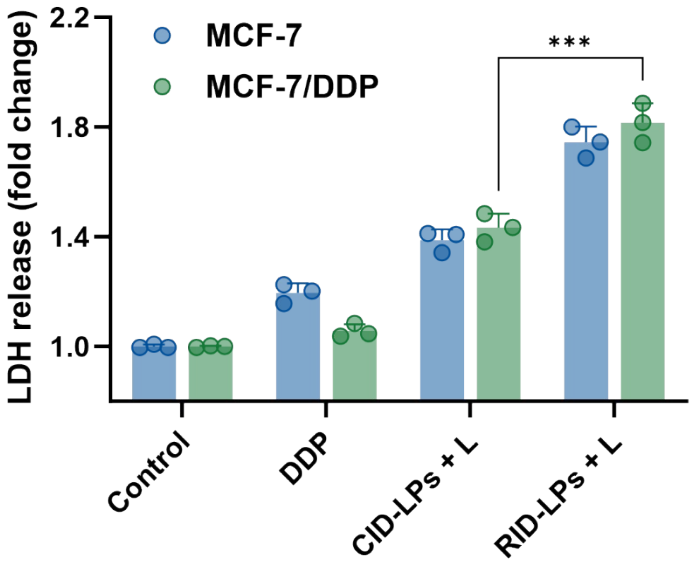

Figure S10. LDH release levels in MCF-7 and MCF-7/DDP cells following treatment with various formulations. (n=3) ***p<0.001; Data are presented as the mean ± SD from three independent experiments; Differences between two groups were assessed by an unpaired t-test, while comparisons among multiple groups were analyzed using one-way ANOVA.

Table S1. Coded and levels of the variables used in Box-Behnken Design (BBD).

Levels	Factors		
	A. Ratio of phospholipid to Rg3	B. Ratio of phospholipid to drugs	C. Ultrasound time (min)
-1	14:2	14:1:1	10
0	14:6	14:3:3	20
1	14:10	14:5:5	30

Table S2. BBD experimental plans and results.

Std.	Factors			Response		
	Ratio of phospholipid to Rg3	Ratio of phospholipid to drugs	Ultrasound time (min)	EE (Rg3)	EE (DDP)	EE (ICG)
1	14:2	14:1:1	20	60.88%	10.64%	73.98%
2	14:10	14:1:1	20	53.86%	41.22%	71.52%
3	14:2	14:5:5	20	55.21%	42.20%	70.87%
4	14:10	14:5:5	20	52.17%	45.76%	44.41%
5	14:2	14:3:3	10	67.26%	31.10%	67.65%
6	14:10	14:3:3	10	62.45%	48.53%	63.45%
7	14:2	14:3:3	30	52.45%	25.53%	76.71%
8	14:10	14:3:3	30	59.28%	48.80%	42.00%
9	14:6	14:1:1	10	54.21%	19.89%	77.43%
10	14:6	14:5:5	10	60.74%	40.29%	79.30%
11	14:6	14:1:1	30	57.92%	16.01%	78.39%
12	14:6	14:5:5	30	56.38%	18.33%	66.08%
13	14:6	14:3:3	20	76.89%	66.09%	80.82%
14	14:6	14:3:3	20	79.88%	65.95%	80.37%
15	14:6	14:3:3	20	74.74%	63.75%	82.49%
16	14:6	14:3:3	20	76.85%	67.70%	85.73%
17	14:6	14:3:3	20	77.47%	67.41%	85.59%

Table S3. Optimum conditions for the preparation of the liposomes as determined by BBD.

Factors		
A. Ratio of phospholipid to Rg3	B. Ratio of phospholipid to drugs	C. Ultrasound time (min)
14:7.1	14:3.6:3.6	22.5

Table S4. Encapsulation efficiency and drug loading capacity of CID-LPs and RID-LPs.

	CID-LPs			RID-LPs		
	Rg3	ICG	DDP	Rg3	ICG	DDP
Encapsulation efficiency (%)	N/A	88.60 ± 1.25	45.08 ± 1.82	96.54 ± 1.13	94.49 ± 1.56	48.56 ± 2.14
Drug loading capacity (%)	N/A	7.41 ± 0.16	14.13 ± 0.31	7.47 ± 0.12	9.92 ± 0.23	14.45 ± 0.42

Note: N/A, not available (Rg3 was not loaded in CID-LPs). All values are expressed as mean ± standard deviation from three independent experiments (n=3).

Table S5. Compositional analysis and formulation parameters of CID-LPs and RID-LPs.

	CID-LPs	RID-LPs
Lecithin (mg)	14.0	14.0
Cholesterol (mg)	7.1	N/A
Rg3 (mg)	N/A	7.1
DSPE-PEG_{2000} (mg)	2.0	2.0
ICG (mg)	3.6	3.6
DDP (mg)	3.6	3.6
Hydration volume (mL)	8.0	8.0
Final concentration of Rg3 (μg/mL)	N/A	856.8 ± 10.0
Final concentration of ICG (μg/mL)	398.7 ± 5.6	425.2 ± 7.0
Final concentration of DDP (μg/mL)	202.9 ± 8.2	218.5 ± 9.6

Note: N/A, not available. All values are expressed as mean ± standard deviation from three independent experiments (n=3).

Table S6. Particle size distribution, polydispersity index, zeta potential of CID-LPs and RID-LPs.

No.	CID-LPs			RID-LPs		
	Size (d.nm)	PDI	Zeta potential (mV)	Size (d.nm)	PDI	Zeta potential (mV)
1	94.5	0.203	-11.2	99.2	0.107	-18.4
2	93.3	0.191	-12.4	100.4	0.131	-21.1
3	91.6	0.178	-14.6	100.2	0.150	-22.6
Mean	93.1	0.191	-12.7	99.9	0.129	-20.7
SD	1.4	0.013	1.7	0.6	0.022	2.1

References

1 T. Chang, Q. Qiu, A. Ji, C. Qu, H. Chen and Z. Cheng, *Biomaterials*, 2022, **287**, 121670.

2 S. Li, Q. Deng, Y. Zhang, X. Li, G. Wen, X. Cui, Y. Wan, Y. Huang, J. Chen, Z. Liu, L. Wang and C. Lee, *Adv. Mater.*, 2020, **32**, 2001146.